NANO LETTERS

2001
Vol. 1, No. 3
121−124

Calculation of the Infrared Optical Transitions in Semiconductor Ellipsoidal Quantum Dots

G. Cantele,* D. Ninno, and G. Iadonisi

INFM and Dipartimento di Scienze Fisiche, Università di Napoli "Federico II", Complesso Universitario M. S. Angelo, via Cintia, I-80126, Naples, Italy

Received December 11, 2000

ABSTRACT

We report on our effective mass calculations for a particle confined in an ellipsoidal quantum dot. Upon using a curvilinear coordinates system, the single particle exact eigenvalues and eigenfunctions have been numerically calculated. Dielectric image effects have been properly taken into account. It is shown that on keeping the volume constant, the confinement energies depend only on the dot shape. The implications of this shape dependence are analyzed for the infrared optical properties.

There is no doubt that semiconductor quantum dots are interesting for both the fundamental physics[1,2] and for novel device applications.[3,4] Quantum confinement and the actual structure shape play a very important role in determining their physical and chemical properties both for open[5] and closed structures.[6−8] Calculations based on the effective mass approximation[1,2] give, for their relative simplicity, an opportunity of studying quantum confinement in those semiconductor nanostructures whose shape differs from the usual spherical and cylindrical ones.[9−12] However, it is necessary to stress that there are a number of circumstances where the effective mass approximation may lead to erroneous results. Pseudopotential calculations have shown that in low dimensional systems one may have instances where the mixings between different conduction band valleys[13,14] and valence bands degeneracy[15] play a fundamental role in determining certain linear and nonlinear optical properties. At the same time, it is well established that when a nanocrystal (a) has a well passivated surface, (b) does not have significant deviations from the bulk lattice structure, (c) it is not too small,[1] and (d) the boundary conditions[16] are chosen with care, band mixings and curvature effects[17,18] for states derived from the zone center conduction band are unlikely to improve significantly the infrared properties we are going to present.

We are going to show that for an ellipsoidal quantum dot the description of the confinement energies as scaling with the dot volume is incorrect if the actual dot shape is not taken into account. Using a proper curvilinear coordinates system in which the Schrödinger equation is separable, we show that the separated differential equations can be solved numerically and the entire exact dot energy spectrum calculated.

We believe that one of the most interesting advances in the science of quantum dots is the availability of colloidal semiconductor nanocrystals where shape control[19] and doping[20] have been achieved. In all the cases, the dots must be embedded in a surface passivating medium that may have a static dielectric constant very different from that of the dot material. The dielectric contrast induces significant dielectric self-energy effects that we have taken into account as a first-order correction. Our calculations will show that, as far as intraband infrared transitions are concerned, there is an almost complete compensation between the dielectric corrections to the ground and first excited states, resulting in a transition energy that is independent from the passivating medium dielectric constant.

Finally, intraband dipole matrix elements have been calculated for a range of ellipsoid eccentricities and the corresponding selection rules discussed.

Theory

The exact solution of the Schrödinger equation for a particle confined in an ellipsoidal quantum dot with hard wall boundary conditions can be calculated using a suitable coordinates system (ξ,η,φ) in which this equation is separable and the boundary (that is, the ellipsoid surface) is represented by an equation like $\xi =$ constant. Let us consider an ellipsoid and indicate with a, b, and c its semi-axes along the x, y, and z directions, respectively (in the following (x, y, z) will represent orthogonal Carthesian coordinates). Let us suppose that it has rotational symmetry around the z axis, namely

* Corresponding author. E-mail: cantele@na.infn.it.

10.1021/nl0055310 CCC: $20.00
Published on Web 02/23/2001

that $a = b$. If $\chi = c/a > 1$ (*prolate* ellipsoid) we introduce the following coordinates transformation (*prolate spheroidal coordinates*):

$$\begin{cases} x = f\sqrt{\xi^2 - 1}\sqrt{1 - \eta^2}\cos\varphi \\ y = f\sqrt{\xi^2 - 1}\sqrt{1 - \eta^2}\sin\varphi \\ z = f\xi\eta \end{cases} \quad (1)$$

where f is a constant, $1 \le \xi < +\infty$, $-1 \le \eta \le 1$, and $0 \le \varphi < 2\pi$. On varying ξ, this transformation parametrizes the space with prolate ellipsoids with semi-axes $f\sqrt{\xi^2-1}$ and $f\xi$ (in the $x-y$ plane and along the z axis, respectively), all having the same focal distance $2f$. This means that the quantum dot ellipsoidal surface is represented by the equation $\xi = \bar{\xi}$, provided that $2f$ is just its focal distance. It is not difficult to show[10] that $f = ce$ and $\bar{\xi} = 1/e$ where $e = \sqrt{1-1/\chi^2}$ is the ellipsoid eccentricity. Writing the Laplacian operator in this new coordinates system, the solution of the Schrödinger equation can be factorized in the form $\Psi_{n,l,m}(\xi,\eta,\varphi) = je_{n,l,m}(\xi)S_{l,m}(\eta)\exp(im\varphi)$, where the rotational symmetry around the z axis has been taken into account. $je_{n,l,m}(\xi)$ and $S_{l,m}(\eta)$ are the respective solutions of the equations

$$\frac{d}{d\xi}\left[(\xi^2 - 1)\frac{d}{d\xi}je(\xi)\right] - \left(A - h^2\xi^2 + \frac{m^2}{\xi^2 - 1}\right)je(\xi) = 0 \quad (2a)$$

$$\frac{d}{d\eta}\left[(1 - \eta^2)\frac{d}{d\eta}S(\eta)\right] + \left(A - h^2\eta^2 - \frac{m^2}{1 - \eta^2}\right)S(\eta) = 0 \quad (2b)$$

which are formally equal but must be solved in different ranges of the respective variables. A is a separation constant while $h = f\sqrt{\epsilon^\nu}$, $\epsilon^\nu = (2m^*/\hbar^2)E$, m^* is the particle effective mass, and E is the volume-confined particle energy. It is found that for most values of A the solution of eq 2b is regular at $\eta = +1$ but not at $\eta = -1$. This means that for each fixed value of h and m there is a discrete set of values of A that correspond to a regular solution in all the range of values of η. We will indicate these values with $A_{l,m}(h)$. Therefore, we have used eq 2b to determine numerically these values and used them in eq 2a. Solving numerically this last one with the boundary condition $je(\bar{\xi}) = 0$ and with fixed l and m, we find a discrete set of values of h that give the volume-confined particle eigenvalues. If we label this set by an index n, these eigenvalues will depend on n, l, and m. Therefore, we can write $E \equiv E_{n,l,m}$, and this justifies the reason for which the eigenfunctions have been labeled in the way indicated previously.

Let us note that, differently from the case of the spherical quantum dot, only n and m represent good quantum numbers (in fact, n is the principal quantum number and $m\hbar$ is the z-component of the particle angular momentum), while l is no longer related to the particle total angular momentum. However, it can be seen that as $\chi \to 1$ eqs 2a and 2b reproduce the spherical quantum dot spectrum. In particular, we have that $A_{l,m}(h) \to l(l+1)$ (independent from h), which means that $l(l+1)\hbar^2$ represents the total particle angular momentum only in this limit. Let us note that $n = 1, 2, 3, \ldots$, $l = 0, 1, 2, \ldots$, and $m = -l, \ldots, 0, \ldots, l$ and that the eigenstates are eigenfunctions of the parity operator too, as a consequence of the system reflection symmetry. Therefore, if we want to look for selection rules for light-induced transitions, we have to take into account both the state parity given by $(-1)^l$ and its angular momentum z-component.

Results and Conclusions

In this section we want to show how, starting from the theoretical background presented in the last section, we can predict several interesting properties of ellipsoidal quantum dots, looking in particular at the role that the system anisotropy can have on the optical infrared transitions.

Solving numerically eqs 2a and 2b using a standard midpoint shooting method, we have determined the exact single particle volume-confined energies for the ground state and several excited states. In Figure 1a we show the confinement energies of the ground state ($n = 1$, $l = 0$, $m = 0$), and of the first five excited ones ($n = 1$, $l = 1$, $m = 0$, ±1 and $n = 1$, $l = 2$, $m = 0$, ±1, ±2), calculated for electrons in CdSe ($m^* = 0.13m_e$) keeping the structure volume constant ($V = 905$ nm^3 corresponding to a sphere with a 6 nm radius). In Figure 1b the transition energies of the first two allowed transitions from the ground state (100 $\to$ 110, full line and 100 $\to$ 11 $\pm$ 1, dashed line) are shown. On increasing χ we are considering structures that are more and more anisotropic obtained by increasing the c axis and decreasing the a axis in such a way that the volume is constant. Although the volume does not change, we can see that the energy levels depend on χ. In particular, the ground-state energy shows a minimum for the spherical shape ($\chi = 1$), being an increasing function of the anisotropy. Another consequence of the anisotropy is the splitting between the states with the same n and l but different values of $|m|$ (as expected because of the loss of rotational symmetry around an arbitrary axis), the only degeneration being with respect to the sign of m. Moreover, we can see that the states with $n = 1$, $l = 0$, $m = 0$, $n = 1$, $l = 1$, $m = 0$ and $n = 1$, $l = 2$, $m = 0$ become degenerate as $\chi \to +\infty$. The same happens for the states with $n = 1$, $l = 1$, $m = \pm1$ and $n = 1$, $l = 2$, $m = \pm1$. This is because in this limit we get a quantum rod with smaller and smaller radius and greater and greater length. For a long quantum rod the confinement energies depend only on the z-component of the angular momentum (that is, m) and the number of nodes of the wave function with respect to the radial coordinate (that is, $n - 1$). This means that, in the considered limit, all the states with the same n and m and different l become degenerate. This explains also the fact that some accidental degeneracies occur, as for example, between the states with $n = 1$, $l = 1$, $m = \pm1$ and $n = 1$, $l = 2$, $m = 0$, because starting from the spherical quantum dot energy levels we must obtain the quantum rod energy levels that have a different order. This is an important conceptual point because it shows how the anisotropy controls the energy levels degeneracies. We can

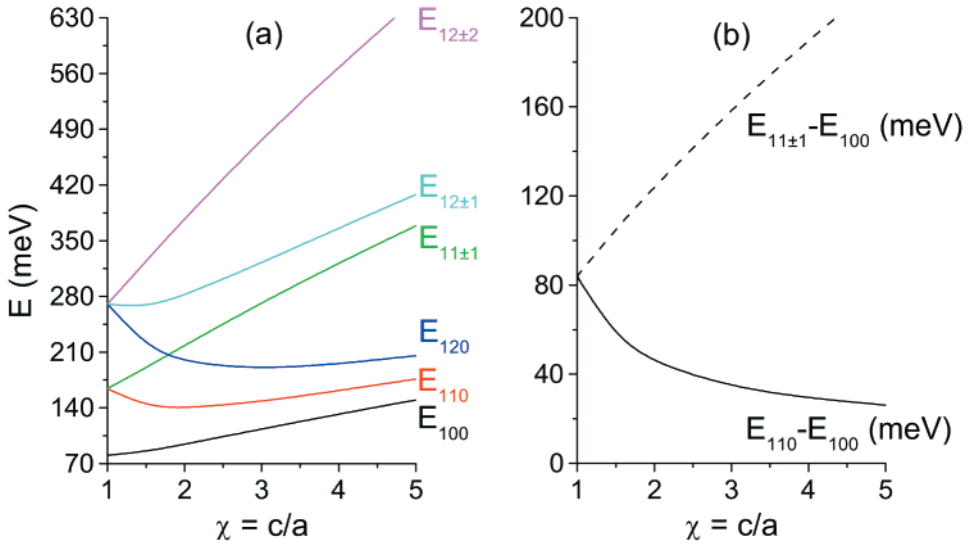

Figure 1. (a) Confinement energies calculated for the ground state and the first five excited states. The structure volume is kept constant at 905 nm^3 corresponding to a sphere with a 6 nm radius. (b) Transition energies for the first (full line) and second (dashed line) allowed transition from the ground state.

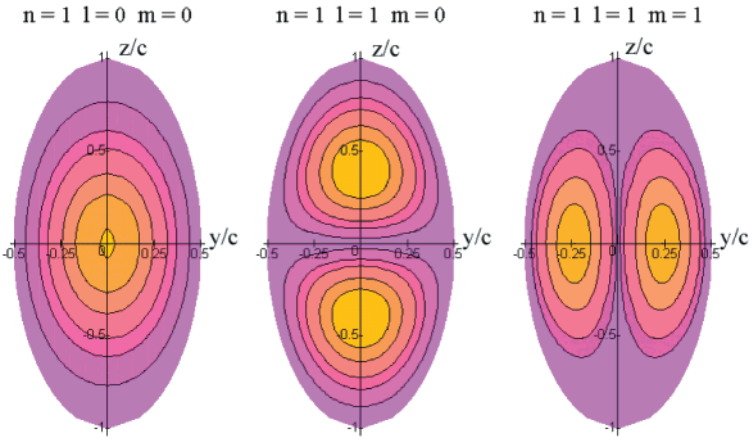

Figure 2. Contour plot for the ground state and two excited states wave function square modulus calculated for $\chi = 2.0$. The yellow regions correspond to the maximum of the probability density.

conclude that the transition energies are strongly dependent on the anisotropy, showing (as Figure 1b clearly demonstrates) the possibility of being tuned by varying the dot shape, keeping its volume constant.

In Figure 2 we show the wave function square modulus for the ground and two excited states, calculated for $\chi = 2.0$. While for the spherical quantum dot the ground state does not depend on the angular coordinates, we observe in this case elliptical contour levels. This "angular distortion" appears for the two excited states too, in such a way that the state with $n = 1$, $l = 1$, $m = 0$ becomes localized around the ellipsoid major axis while the one with $n = 1$, $l = 1$, $m = \pm 1$ is localized around the minor axis. This is an important difference with respect to the spherical quantum dot, which, as we are going to see, has some consequences for the system optical properties.

The single particle energies shown previously have been calculated by neglecting the image dielectric effects. It is known that a particle moving through a medium of dielectric constant ε_r embedded in an external medium of dielectric constant $\varepsilon_{ext} \neq \varepsilon_r$ polarizes its surroundings. As a result, a surface polarization charge appears, giving rise to a dielectric potential that acts on the particle itself. In that sense we can speak of dielectric self-energy. It is possible that taking into account these effects, the single particle levels can change and the infrared optical transition energies be modified with respect to the case $s \equiv \varepsilon_r/\varepsilon_{ext} = 1$. Therefore, we have evaluated to the first order of the perturbation theory these effects by calculating exactly the self-polarization potential and evaluating its mean value on the quantum states previously discussed. In Figure 3 we show the corrections to the ground state (full curve) and to the first excited one (dashed curve), calculated for CdSe ($\varepsilon_r = 10$) as a function of s. The ellipsoid axes have been fixed at $c = 5$ nm and $a = 4.2$ nm ($\chi = 1.2$). The correction for the second excited state is not shown because it is in practice coincident with that of the first excited state. In the same figure the single particle levels are also shown to give a better understanding on how these dielectric effects can influence the infrared transitions. It comes out that the correction to a given level

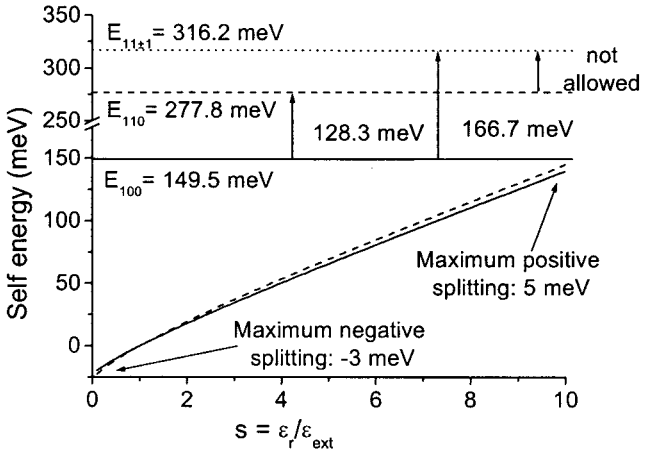

Figure 3. Image dielectric effects calculated for CdSe. The single particle energy level shifts are shown for the ground state (full curve) and the first excited one (dashed curve). The correction to the second excited state is in practice coincident with this last one. The energy levels calculated neglecting these effects are also shown for comparison. The ellipsoid axes have been fixed at $c = 5$ nm and $a = 4.2$ nm ($\chi = 1.2$).

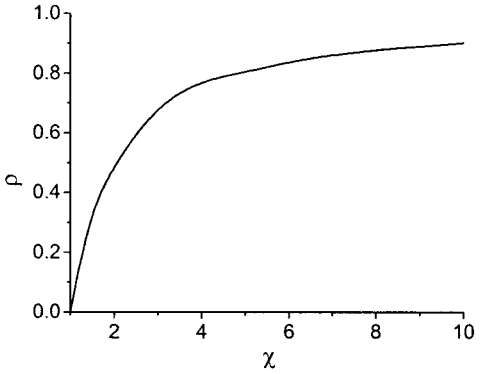

Figure 4. Polarization anisotropy as a function of χ. It comes out that the system response to light circularly polarized in the plane orthogonal to the major axis becomes less efficient than the response to light linearly polarized along that axis as the dot anisotropy increases.

is quite significant as s increases. Nevertheless, if we consider the energy differences between these levels, the correction becomes negligible. This means that embedding the dot in media with a different dielectric constant, significant variation of the infrared optical transition energies should not be observed.

The main effects of the anisotropy are on the system optical properties as seen when studying transition rates between different levels. For example, we have already stressed the different structure of the first two excited states, which should produce interesting effects with respect to absorbed and/or emitted light polarization. In Figure 4, we show the light polarization anisotropy, defined as $\rho = (p_{||} - p_{\perp})/(p_{||} + p_{\perp})$, where $p_{||} = |\langle 110|z|100\rangle|^2$ and $p_{\perp} = |\langle 11 \pm 1|(x \pm iy)/2^{1/2}|100\rangle|^2$ are the optical matrix elements. It is seen that on increasing the anisotropy, the transition toward the state with $n = 1$, $l = 1$, $m = 0$ (allowed with linearly polarized light) becomes more efficient than that toward the states $n = 1$, $l = 1$, $|m| = 1$ (allowed with circularly polarized light), as a consequence of the different structure of the two states.

In conclusion, we have presented some properties of ellipsoidal quantum dots, with particular reference to the influence of the structure shape on the optical transitions. The results show a strong dependence of the optical transition energies on the system anisotropy, as well as a shape-dependent response to polarized light. Image dielectric effects have been investigated for infrared transitions, showing that the transition energies are in practice not affected by these effects.

Acknowledgment. G.C. has been supported by the European Social Fund. Financial support from ENEA under contract No. 2000/29324 is acknowledged.

References

(1) Brus, L. *J. Phys. Chem.* **1986**, *90*, 2555.
(2) Yoffe, A. D. *Adv. Phys.* **1993**, *42*, 173.
(3) Zhuang, L.; Guo, L.; Chou, S. Y. *Appl. Phys. Lett.* **1998**, *72*, 1205.
(4) Grundmann, M. *Physica E* **2000**, *5*, 167.
(5) Cantele, G.; Ninno, D.; Iadonisi, G. *Phys. Rev. B* **2000**, *61*, 13730.
(6) Wang Lin-Wang, Zunger, A. *J. Phys. Chem.* **1994**, *98*, 2158.
(7) Chin-Yu, Y.; Zhang, S. B.; Zunger, A. *Phys. Rev. B* **1994**, *50*, 14405.
(8) Ninno, D.; Iadonisi, G.; Buonocore, F.; Cantele, G.; Di Francia, G. *Sens. Actuators B* **2000**, *68*, 17.
(9) AI. Efros, L.; Rondina, A. V. *Phys. Rev. B* **1993**, *47*, 10005.
(10) Cantele, G.; Ninno, D.; Iadonisi, G. *J. Phys.: Condens. Matter* **2000**, *12*, 9019.
(11) Ninno, D.; Iadonisi, G.; Buonocore, F. *Solid State Commun.* **1999**, *112*, 521.
(12) Buonocore, F.; Ninno, D.; Iadonisi, G. *Phys. Rev. B* **2000**, *62*, 10914.
(13) Ninno, D.; Wong, K. B.; Gell, M. A.; Jaros, M. *Phys. Rev. B* **1985**, *32*, 2700.
(14) Shaw, M. J.; Ninno, D.; Adderley, B. M.; Jaros, M. *Phys. Rev. B* **1992**, *45*, 11031.
(15) Ninno, D.; Gell, M. A.; Jaros, M. *J. Phys. C: Solid State Phys.* **1986**, *19*, 3845.
(16) Braginsky, L. S. *Phys. Rev. B* **1999**, *60*, R13970.
(17) Mizel, A.; Cohen, M. L. *Phys. Rev. B* **1997**, *56*, 6737.
(18) Ekimov, A. I.; Hache, F.; Schanne-Klein, M. C.; Ricard, D.; Flytzanis, C.; Kudryavtsev, I. A.; Yazeva, T. V.; Rodina, A. V.; Al. Efros, L. *J. Opt. Soc. Am. B* **1993**, *10*, 100.
(19) Xiaogang, P.; Manna, L.; Weidong Yang, Wickham, J.; Scher, E.; Kadavanich, A.; Alivisatos, A. P. *Nature* **2000**, *404*, 59.
(20) Shim, M.; Guyot-Sionnest, P. *Nature* **2000**, *407*, 981.

NL0055310